NJC

Accepted Manuscript

This is an *Accepted Manuscript*, which has been through the Royal Society of Chemistry peer review process and has been accepted for publication.

Accepted Manuscripts are published online shortly after acceptance, before technical editing, formatting and proof reading. Using this free service, authors can make their results available to the community, in citable form, before we publish the edited article. We will replace this *Accepted Manuscript* with the edited and formatted *Advance Article* as soon as it is available.

You can find more information about *Accepted Manuscripts* in the Information for Authors.

Please note that technical editing may introduce minor changes to the text and/or graphics, which may alter content. The journal's standard Terms & Conditions and the Ethical guidelines still apply. In no event shall the Royal Society of Chemistry be held responsible for any errors or omissions in this *Accepted Manuscript* or any consequences arising from the use of any information it contains.

ROYAL SOCIETY OF CHEMISTRY

www.rsc.org/njc

Formation and corrosion resistance of phosphate chemical conversion coating on medium carbon low alloy steel

Cong-cong Jiang[a,b,c], Gui-yong Xiao[a,b,c], Xian Zhang[a,b,c], Rui-fu Zhu [a,b,c*], Yu-peng Lu[a,b,c**]

[a] Key Laboratory for Liquid-Solid Structural Evolution and Processing of Materials, Ministry of Education, Shandong University, Ji'nan, 250061, China;

[b] School of Materials Science and Engineering, Shandong University, Ji'nan, 250061, China;

[c] Suzhou Institute, Shandong University, Suzhou, 215123, China

Abstract

Chemical conversion coatings have attracted more attention in recent years due to their excellent characteristics such as corrosion resistance, wear resistance, adhesion and lubrication. In this study, phosphate chemical conversion (PCC) coating was fabricated on medium carbon low alloy steel by the facile PCC method with the addition of Fe^{2+} curing process at room temperature. It is shown that the coating was composed of hopeite ($Zn_3(PO_4)_2{\cdot}4H_2O$) and minor phosphophyllite ($Zn_2Fe(PO_4)_2{\cdot}4H_2O$) in the form of fine and flaky crystals along the direction inclined or perpendicular to substrate surface. Adhesive test indicated that the PCC coating was strongly attached on the substrate. The electrochemical analysis revealed that the as-prepared coating imparted better corrosion resistance to the steel substrate.

Keywords: Alloy steel; Phosphate chemical conversion; Corrosion resistance

1. Introduction

As an important class of steels, medium carbon low alloy steel has been widely

* Corresponding author: Tel: 86-0531-88395966; Fax: 86-0531-88395966. E-mail address: ruifuzh@sdu.edu.cn(R. F. Zhu)

** Corresponding author: Tel: 86-0531-88395966; Fax: 86-0531-88395966. E-mail address: biosdu@sdu.edu.cn (Y. P. Lu)

used in aerospace and appliance industries due to its workability and excellent mechanical performances. However, its corrosion behavior has been commonly observed in aggressive medium, which can lead to corrosion and failure[1, 2]. Therefore, concerns arise significantly in the surface modification to endow the steel with a protective coating. So far, there have been a variety of surface treatments adopted on steels, such as plasma spraying [3], electroless plating [4], electroplating [5], and ion implantation methods [6].

In many cases, phosphate chemical conversion (PCC) is regarded as an ideal way, which shows advantages such as low-cost, rapid coating formation and suitability for treatment of irregular surfaces[7-9]. This method plays a significant role in industry, due to its excellent corrosion resistance, wear resistance, adhesion of the underlying substrate, etc. The PCC baths are classified as zinc, manganese, iron, calcium, magnesium and chromate systems, which is based on the nature of the metal ion constituting the major component of the PCC bath. Especially, the main composition of zinc PCC coatings on steel substrates are hopeite ($Zn_3(PO_4)_2{\cdot}4H_2O$) and phosphophyllite ($Zn_2Fe(PO_4)_2{\cdot}4H_2O$) with excellent corrosion resistance [9, 10]. For decades, PCC treatment has been specified as a good choice for a large percentage of steel and iron ordnance components which need excellent corrosion resistance[11-13].

It is reported that the presence of alloying elements and their chemical nature cause distinct difference in phosphate ability[11]. Meanwhile, low carbon steels undergo phosphating easily and produce superior quality coating, while phosphate rate becomes slower and the resultant crystals are larger with increased carbon content [7]. Usually, high temperature phosphating are adopted to fabricate PCC coatings on medium carbon low alloy steel. For example, Arun Kumar et al[12] studied zinc phosphated medium carbon low alloy steel using high temperature phosphating bath

(90 ℃) and found that the layer of phosphate coating consisted of numerous crystals of very different sizes. While the low or room temperature phosphating will become one inevitable trend to overcome the energy crisis, the room temperature phosphating technique has shortcomings including low phosphorization speed, thin coating and poor corrosion resistance [14]. Therefore, it is usually difficult to deposit a high quality phosphate coating on medium carbon low alloy steel at room temperature.

In this paper, we reported the fabrication of the fine-crystalline and uniform PCC coating on 35CrMnSi steel by the PCC method at room temperature. The effect of Fe^{2+} curing on the microstructure of PCC coating as well as the adhesive strength and corrosion resistance were investigated.

2. Materials and method

2.1. Chemical conversion process

In the present study, 35CrMnSi steel (of 10 mm×10 mm×3 mm dimensions) of the following composition was used as substrate: 0.35 wt% C, 1.16 wt% Si, 0.82 wt% Mn, 1.17 wt% Cr, 0.01 wt% S, 0.022 wt% P and balance Fe. The samples were abraded using emery paper, followed by degreasing in NaOH solution. Then, pickling was performed on samples. Afterwards, activation was conducted in a solution of Ti colloids ($Na_4TiO(PO_4)_2$, commercially obtained) at room temperature. The samples were then immersed in a PCC bath at room temperature for different times. The PCC bath was composed of zinc oxide (10 ~ 25 g/L), phosphoric acid (5 ~ 15 mL/L), nitric acid (20 ~ 30 mL/L) and accelerant (1 ~ 2.5 g/L), with the pH value of 2.75. Before the immersion process, the bath solution was cured with a 5 g/L pure iron powder at room temperature for 12 h. After curing, the remaining pure iron powder was removed. Finally, the coupons were washed with distilled water and dried by blowing air at room temperature.

2.2. Phase and microstructure characterization

The microstructure of coating was studied using a SU-70 Field Emission SEM (FE-SEM). The phase analysis of the coatings was carried out by a Rigaku D/max-γB X-ray diffractometer (XRD) using CuKα radiation, operated at 40 kV and 100 mA with a scan speed of 4 °/min.

2.3. Scratch test

Scratch adhesion test was performed on the surface of coating by using a commercial automatic scratch tester equipped with a diamond stylus (cone apex angle 120 °, tip radius 200 um) and an acoustic emission monitoring system to detect acoustic emission from crack formation. Scratches were made under stepwise increasing load for an interval length of 4 mm. The increased load was applied from 0 to 70 N at a load rate of 35 N $\cdot$mm^{-1} with a sliding speed of 2 mm $\cdot$min^{-1}. The results of critical normal load were the average value of five different measurements.

2.4. Electrochemical measurements

The corrosion characteristic of the coating was investigated by potentiodynamic polarization tests with a three-electrode setup in 3.5 wt% NaCl aqueous solution, at a scan rate of 5 mV/s. The saturated calomel electrode (SCE), platinum, and the sample coupon with 1 cm^2 exposed area were used as reference, counter, and working electrodes in the three-electrode cell (Parstat 2273), respectively. All EIS measurements were conducted at an open circuit potential (OCP) after reaching a steady state, with voltage perturbation amplitude of 5 mV and a frequency range from 100 kHz to 0.01 Hz.

3. Results and discussion

The PCC coating on 35CrMnSi steel was fabricated by immersed in a PCC bath at room temperature. The PCC bath with the addition of Fe^{2+} curing process was

composed of zinc oxide, phosphoric acid, nitric acid and accelerant, with the pH value of 2.75. The microstructure, phase, adhesion strength and corrosion resistance were characterized as follows.

3.1. Microstructure characterization

Fig.1 shows the FE-SEM images of PCC coatings obtained in room temperature bath for 15 min with and without the addition of Fe^{2+} curing process. It was observed that a well-crystallized and dense coating fully covered the both substrates, and the most crystals grew along the direction inclined or perpendicular to substrate surface. Further, it can also be clearly seen that the coating with Fe^{2+} curing was composed of fine and flaky crystals with size of about 2 ~ 5 μm, which was significantly less than that of the conventional PCC coating without Fe^{2+} curing with a crystal size of about 50 ~ 60 μm.

In general, the formation rate of PCC coating on steels depended on the concentration of Fe^{2+} on the interface between the PCC bath and substrate which increased the number of active centers and thus decreased the crystal size markedly[7]. A high enough concentration of Fe^{2+} could initiate the chemical conversion reactions and accelerate the formation of PCC coating. Besides, the presence of Fe^{2+} in bath was beneficial to the formation of phosphophyllite ($Zn_2Fe(PO_4)_2 \cdot 4H_2O$) in coating which had good corrosion resistance due to its chemical stability[10].

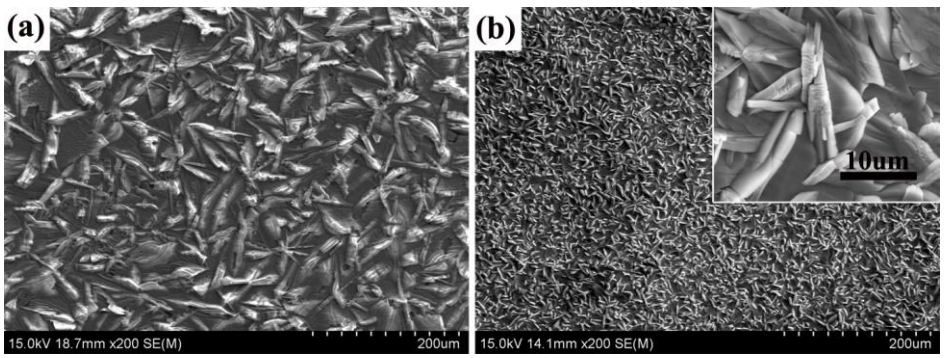

Fig. 1 FE-SEM images of PCC coatings obtained in bath for 15 min (a) without and (b) with the addition of Fe^{2+} curing process.

It has been demonstrated recently that the grain boundaries drastically changed the properties of the coatings, they strongly depended on the presence of defects like interphase boundaries and grain boundaries[15, 16]. The corrosion of PCC coating started from the defects like interphase boundaries and grain boundaries with higher energy and lower stability compared with free surfaces. However, the grain size had a larger impact on the corrosion resistance of coatings. Usually, the homogeneous fine-crystalline coating with high compactness and low porosity had excellent corrosion resistance, which can usually be used for anti corrosion applications. While the coarse-crystalline coating with high porosity can be acted as base for paint applications. In this research, we intended to highlight the application of corrosion resistance of PCC coating, thus the fine-crystalline coating with Fe^{2+} curing were discussed in detail in the following sections.

The FE-SEM images of PCC coatings obtained in bath for different times with Fe^{2+} curing process were shown in Fig. 2. When the steel substrate was PCC treated for 3 min, many small plate-like crystals were formed on substrate surface, and the plate-like crystals were embedded in substrate (Fig. 2a). When the PCC treatment was conducted for 5 and 8 min, the crystals grew quickly to form bigger crystals, and some new small crystal grains formed on the bigger ones, while the substrate was not fully covered by PCC coating (Fig. 2b-c). When it came to 10 min, the crystals packed like leaves and finally a complete, dense coating on the surface was formed (Fig. 2d).

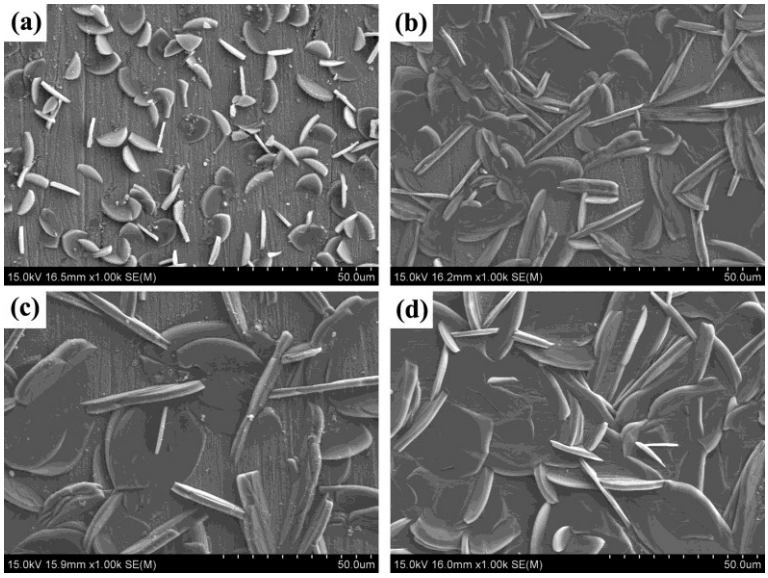

Fig. 2 FE-SEM images of PCC coatings obtained in bath for (a) 3 min, (b) 5 min, (c) 8 min and (d) 10 min with Fe^{2+} curing process.

From the growth process of PCC coating at different times, especially at the early age of growth process, it can be seen that the plate-like crystals were embedded in substrate, which indicated the substrate involved in the chemical reaction of PCC coating formation. Literatures[7, 14, 17] have explained some possible PCC reactions on steels in zinc phosphate solution. Specifically, when substrate was immersed into the PCC bath, iron dissolved at the micro anodes through the following reaction:

$$Fe + 2H^+ \rightarrow Fe^{2+} + H_2\uparrow \quad (1)$$

Hydrogen evolution occurred at the micro cathodic sites resulting in an increase of pH value at the metal/solution interface. This change in pH value altered the dissociation equilibrium, which led to the formation of PO_4^{3-}.

$$H_3PO_4 \rightarrow H_2PO_4^- + H^+ \rightarrow HPO_4^{2-} + 2H^+ \rightarrow PO_4^{3-} + 3H^+ \quad (2)$$

When PO_4^{3-} run into Fe^{2+}, ferrous phosphate as a subcrystalline layer was rapidly formed in the case of steel, on which crystalline layer of phosphates built up in future.

$$2PO_4^{3-} + 3Fe^{2+} + 8H_2O \rightarrow Fe_3(PO_4)_2 \cdot 8H_2O\downarrow \quad (3)$$

Whilst PO_4^{3-} and metal ions (Zn^{2+}, Fe^{2+}) in the bath reached saturation, the deposition of insoluble phosphate would be achieved. Then it can be crystallized into

PCC coating on a subcrystalline layer.

$$2Zn^{2+} + Fe^{2+} + 2PO_4^{3-} + H_2O \rightarrow Zn_2Fe(PO_4)_2 \cdot 4H_2O\downarrow \quad (4)$$

$$Zn^{2+} + 2PO_4^{3-} + 4H_2O \rightarrow Zn_3(PO_4)_2 \cdot 4H_2O\downarrow \quad (5)$$

In summary, the PCC coating was formed on substrate via complicated chemical and electrochemical reactions, which caused the substrate surface to integrate itself as a part of the PCC coating. Therefore, the PCC coating was considered to be highly adherent to the substrate, which will be confirmed by the scratch adhesion test in section 3.3. Moreover, the resultant coating with the composition of hopeite and phosphophyllite can protect substrate by providing an insulator barrier between the metal and environment, which will be also discussed in section 3.4 in detail.

3.2. Phase composition

Fig. 3 shows the XRD pattern of PCC coating obtained in bath for 15 min with Fe^{2+} curing process. As can be seen, the coating was mainly composed of hopeite ($Zn_3(PO_4)_2 \cdot 4H_2O$) with minor phosphophyllite ($Zn_2Fe(PO_4)_2 \cdot 4H_2O$). It is reported that hopeite possessed excellent rust resistance and water tolerance, and thus can be widely used as anti rust paints. Furthermore, phosphophyllite had better corrosion resistance than that of hopeite due to its chemical stability[10]. Meanwhile, there also existed amorphous phase clearly shown in the inset of Fig. 3. As previously reported, the growth of phosphate coating was initiated by the formation of a subcrystalline layer (ferrous phosphate) on which crystalline layer of phosphates built up rapidly [7]. Thus, it can be deduced that the amorphous phase was most likely to be ferrous phosphate ($Fe_3(PO_4)_2 \cdot 8H_2O$).

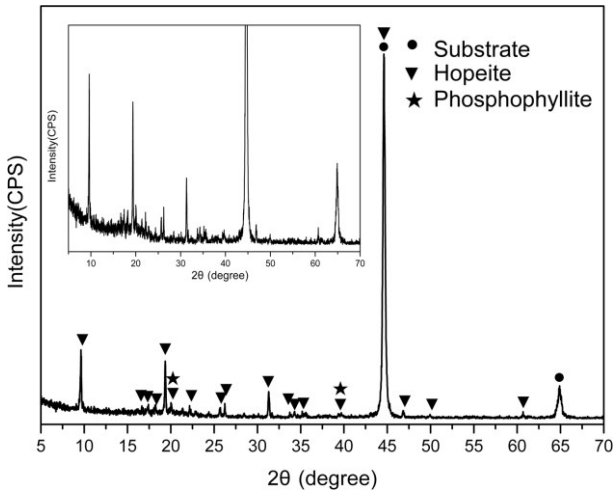

Fig. 3 XRD pattern of PCC coating obtained in bath for 15 min with Fe^{2+} curing process. The inset image showing a higher magnification.

3.3. Adhesion strength

Fig. 4 shows the variation curves of scarification friction/sound-force of PCC coating obtained in bath for 15 min with Fe^{2+} curing process. The adhesion strength was represented by the critical normal load at which a diamond stylus has just come into contact with the substrate. The critical normal load at which flaking occurred was determined by acoustic emission monitoring system from crack formation and sudden change of friction force together[18-20]. According to the result of adhesion test, the determined critical normal load was 50.7 ± 1.8 N. Meanwhile the best curve along with microscope image of the coated sample was showed in Fig. 4. The PCC coating were highly adherent to the underlying metal according to the reports of Sankara [7] and Zhang [10]. As mentioned in section 3.1, the PCC coating was formed on substrate via complicated chemical and electrochemical reactions, which caused the substrate surface to integrate itself as a part of the PCC coating. Thus, the PCC coating was considered to be highly adherent to the substrate, which was demonstrated through the cross-section image of PCC coating (Fig. 5(a)). Fig. 5(b) shows the EDS spectra of coating, indicating that O, Fe, Zn and P were the dominant elements on the surface of

coating. The result was in good agreement with the results of XRD (Fig. 3).

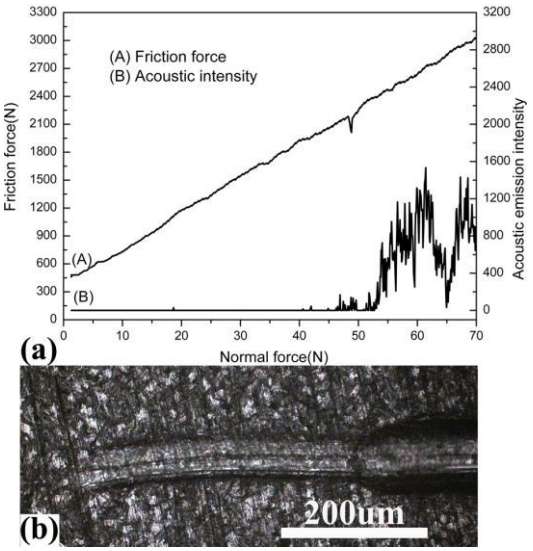

Fig. 4 (a) Variation curves of scarification friction/sound-force and (b) scratch track of PCC coatings obtained in bath for 15 min with Fe^{2+} curing process.

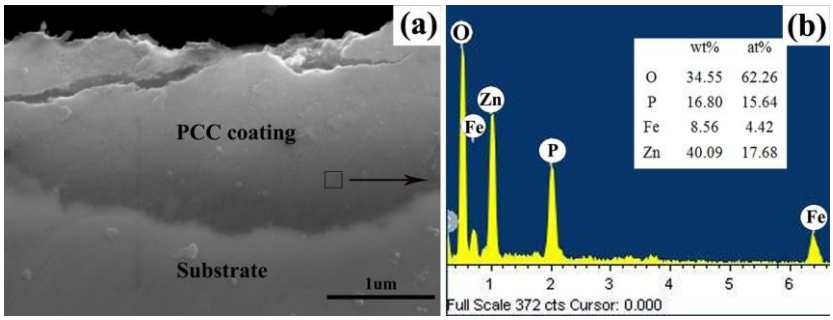

Fig. 5 (a) SEM of the cross-section image along with (b) EDS mapping of the PCC coating obtained in bath for 15 min with Fe^{2+} curing process.

3.4. Electrochemical investigation

3.4.1. Open circuit potential (OCP) and potentiodynamic polarization

The changes of OCP as a function of time for the PCC coating obtained in bath for 15 min with Fe^{2+} curing process and bare substrate in 3.5 wt% NaCl solution are presented in Fig. 6. Generally, a high open-circuit potential value indicated a high tendency to resist to corrosion[21, 22]. The OCP curve of bare substrate displayed a higher shift toward the noble direction as soon as the sample was immersed in the PCC bath and then stabilized close to −650 mV after 820 s. This shift could be due to

the oxidization that occurred at the substrate surface. The OCP of the PCC coating remained more or less constant throughout the test due to the formation of an intact coating on the substrate. Meanwhile, the PCC coating had higher open-circuit potential value than that of substrate, indicating a high tendency to resist to corrosion relative to substrate.

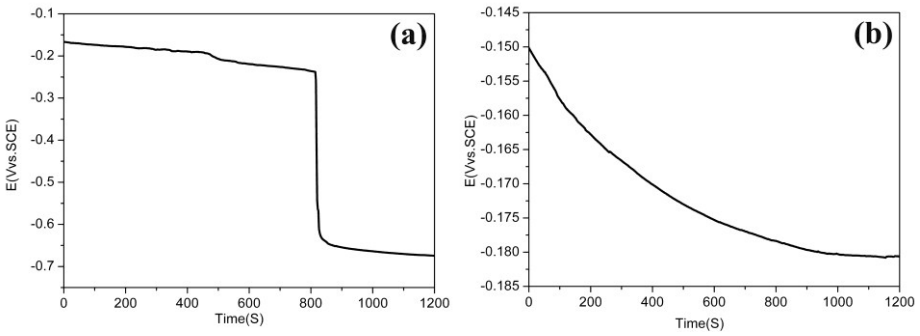

Fig. 6 Variation of OCP as a function of time for (a) substrate and (b) PCC coating obtained in bath for 15 min with Fe^{2+} curing process.

For determination of corrosion resistance, it was not sufficient only to consider the open-circuit potential as determination criterion. The polarization curve and electrochemical impedance spectroscopy were found to be very appropriate to study the entire corrosion resistance.

The potentiodynamic polarization curves for the PCC coating and bare substrate are shown in Fig. 7. As described in section 3.1, the cathodic reaction was corresponding to the evolution of hydrogen, while the anodic polarization curve related to the corrosion resistance of the coating. As a general tendency, the hydrogen evolution is weakened as soon as the samples are immersed in the PCC bath. The electrochemical parameters calculated from the polarization curves by Tafel extrapolation are summarized in Table 1. Corrosion current density (i_{corr}) and corrosion potential (E_{corr}) were used to evaluate the protective property of the coatings. The i_{corr} was correlated with the corrosion rate. A high current density corresponded to a high corrosion rate of the sample[9, 23, 24]. It can be seen that the E_{corr} of PCC coating was approximately

0.58 V positive than that of bare substrate. The i_{corr} of the PCC coating was 2.14 μA cm^{-2}, which was about 10 times lower than that of bare substrate (21.88 μA cm^{-2}). This means that PCC coating endowed the steel excellent corrosion resistance.

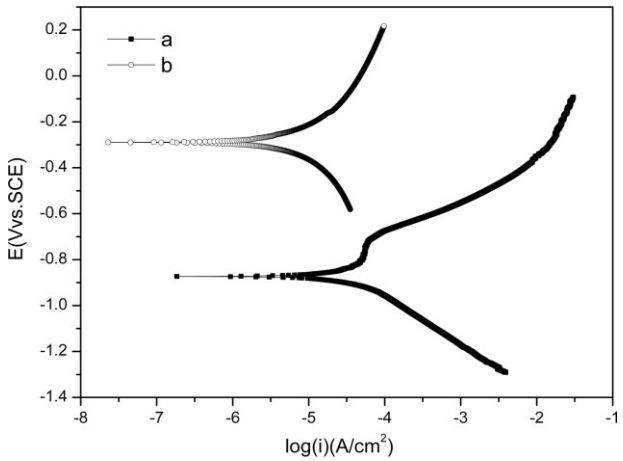

Fig. 7 Potentiodynamic polarization curves for (a) substrate and (b) PCC coating obtained in bath for 15 min with Fe^{2+} curing process.

Table 1 The fitting values of electrochemical parameters of (a) bare steel and (b) PCC coating obtained in bath for 15 min with Fe^{2+} curing process.

Samples	E_{corr} (V_{SCE})	i_{corr} (μA cm^{-2})	R_s ($\Omega \cdot cm^2$)	Y_0 ($\times 10^{-5} \Omega^{-1}$ cm^{-2} S^{-n})	R_{ct} ($k\Omega \cdot cm^2$)	n
a	-0.87	21.88	15.35	79.24	0.58	0.78
	±0.09	±0.27	±2.12	±5.58	±0.04	±0.05
b	-0.29	2.14	18.91	7.77	2.78	0.59
	±0.12	±0.04	±5.81	±2.2	±0.74	±0.09

3.4.2. Electrochemical impedance spectroscopy (EIS)

EIS was also used as an effective tool to determine the electrochemical corrosion behavior of the coating. The EIS results for substrate and PCC coating in 3.5 wt% NaCl solution at OCP are shown in Fig. 7 as Nyquist and Bode diagrams. Fig. 8(a) shows both of specimens were approximately characterized by one large semicircle.

The diameter of the semicircle for PCC coating was larger than that of substrate, indicating a high polarization resistance was obtained for the PCC treated sample[9, 25]. Fig. 8(b) showing the |Z| Bode plot exhibited an increase in impedance value of PCC coating relative to substrate. The increase in the impedance value indicated an increase in corrosion resistance of PCC coating[26, 27]. This phenomenon was indicative of the fact that the PCC coating had a high resistivity in NaCl solution. The Bode plot in phase angle also showed that a large shift in the phase angle toward −90° was observed for PCC coating, as well as an inverse shift that occurred at low frequency. It is reported that the phase angle (−θ) at high frequency was a good criterion for integrity of coating as well as coating degradation in corrosive medium[9, 23]. Hence, an increase in −θ showed the increase in coating intactness. In the present study, the higher phase angle obtained for PCC treated sample at the high frequency region was attributed to the formation of PCC coating over the surface.

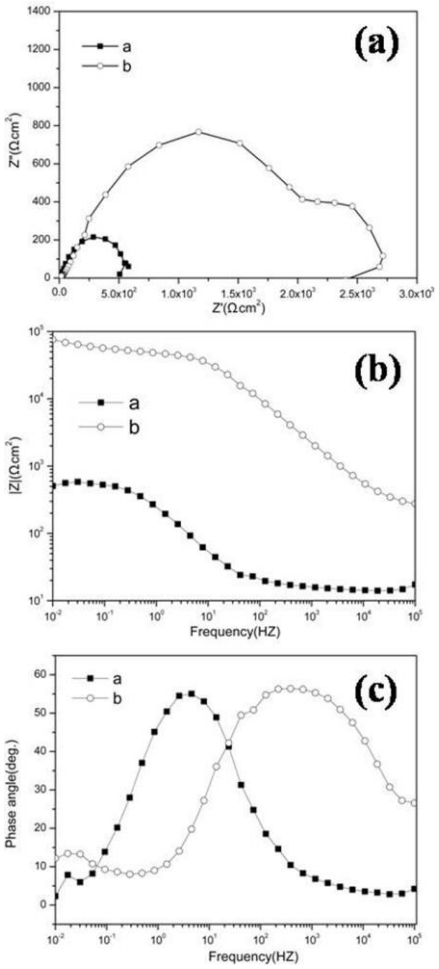

Fig. 8 Impedance spectra presented in (a) Nyquist plot, (b) Bode phase angle, and (c) Bode amplitude plots for (a) substrate and (b) PCC coating obtained in bath for 15 min with Fe^{2+} curing process.

The electrochemical equivalent circuit as shown in Fig. 9 was used for fitting EIS data. The circuit consisted of solution resistance (R_s), charge transfer resistance (R_{ct}) and a constant phase element (CPE) which replaced the capacitance of the double layer (C_{dl}) due to the roughness and inhomogeneity of the electrode surface. The higher charge transfer resistance, the higher corrosion resistance of coating. The values of parameters for the bare substrate and PCC coating extracted from the plot are listed in Table 1. The results showed that the R_{ct} values of PCC coating was 2.78 kΩ cm^{-2} which was about 4 times than that of bare substrate with the R_{ct} of 0.58 kΩ cm^{-2}. The capacitance values of PCC coating was significantly lower than that of

bare substrate. This can be explained by the presence of hopeite and phosphophyllite reducing the susceptibility to corrosion.

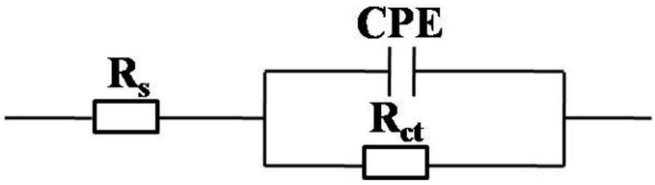

Fig. 9 Equivalent electrical circuits used to model the impedance behavior.

To sum up, it can be concluded that the corrosion resistance of PCC coating was better than that of bare substrate. The better corrosion protection of PCC coating derived from the presence of hopeite and phosphophyllite as an insulator which were not directly engaged in any electrochemical reaction and thus provided a barrier between the substrate and surrounding environment.

4. Conclusion

The fine and dense coating was fabricated on 35CrMnSi steel substrate by the phosphate chemical conversion (PCC) method at room temperature. A high enough concentration of Fe^{2+} could initiate the chemical conversion reactions and accelerate the formation of PCC coating. The coating was mainly composed of hopeite ($Zn_3(PO_4)_2 \cdot 4H_2O$) and minor phosphophyllite ($Zn_2Fe(PO_4)_2 \cdot 4H_2O$) in the form of fine and flaky crystals, along the direction inclined or perpendicular to substrate surface. Adhesive test indicated that the PCC coating was strongly attached on the substrate owing to the surface of substrate as a part of PCC coating via chemical and electrochemical reactions. The electrochemical analysis revealed that the as-prepared coating imparted better corrosion resistance to the steel substrate by providing an insulator barrier between the metal and environment.

Acknowledgements

This work was supported by The Fundamental Research Funds of Shandong

University (2015JC018), Shandong Provincial Natural Science Foundation of China (ZR2013EMM013), Jiangsu Province Science Foundation for Youths (BK20140412) and Science and Technology Development Program of Shandong Province, China (2014GGX102031).

References

1. Y. Li, G. Y. Xiao, L. B. Chen and Y. P. Lu, *Sci. China-Technol. Sci.*, 2013, **56**, 2581-2585.
2. L. Jiao, T. Li, X.-b. Wang, L. Qin and J.-j. Chen, *Trans. Beijing Inst. Technol.*, 2013, **33**, 22-25, 36.
3. A. N. Khan and J. Lu, *Surf. Coat. Technol.*, 2007, **201**, 4653-4658.
4. J. L. Tang and Y. Zuo, *Corrosion Sci.*, 2008, **50**, 2873-2878.
5. N. Imaz, M. Ostra, M. Vidal, J. A. Diez, M. Sarret and E. Garcia-Lecina, *Corrosion Sci.*, 2014, **78**, 251-259.
6. P. Saravanan, V. S. Raja and S. Mukherjee, *Corrosion Sci.*, 2013, **74**, 106-115.
7. T. Narayanan, *Rev. Adv. Mater. Sci.*, 2005, **9**, 130-177.
8. H. Y. Su and C. S. Lin, *Corrosion Sci.*, 2014, **83**, 137-146.
9. X. C. Zhao, G. Y. Xiao, X. Zhang, H. Y. Wang and Y. P. Lu, *J. Phys. Chem. C*, 2014, **118**, 1910-1918.
10. X. Zhang, G. Y. Xiao, Y. Jiao, X. C. Zhao and Y. P. Lu, *Surf. Coat. Technol.*, 2014, **240**, 361-364.
11. L. Fang, L.-b. Xie, J. Hu, Y. Li and W.-t. Zhang, *Physics Procedia*, 2011, **18**, 227-233.
12. A. Kumar, S. K. Bhola and J. D. Majumdar, *Surf. Coat. Technol.*, 2012, **206**,

3693-3699.

13. Y. Totik, *Surf. Coat. Technol.*, 2006, **200**, 2711-2717.

14. H.-Y. Su and C.-S. Lin, *Corrosion Sci.*, 2014, **83**, 137-146.

15. S. G. Protasova, B. B. Straumal, A. A. Mazilkin, S. V. Stakhanova, P. B. Straumal and B. Baretzky, *J. Mater. Sci.*, 2014, **49**, 4490-4498.

16. T. Tietze, P. Audehm, Y. C. Chen, G. Schutz, B. B. Straumal, S. G. Protasova, A. A. Mazilkin, P. B. Straumal, T. Prokscha, H. Luetkens, Z. Salman, A. Suter, B. Baretzky, K. Fink, W. Wenzel, D. Danilov and E. Goering, *Sci. Rep.-UK*, 2015, **5**, 8871.

17. A. S. Akhtar, K. C. Wong and K. A. R. Mitchell, *Appl. Surf. Sci.*, 2006, **253**, 493-501.

18. F. Attar and T. Johannesson, *Surf. Coat. Technol.*, 1996, **78**, 87-102.

19. L. Vieira, F. L. C. Lucas, S. F. Fisssmer, L. C. D. dos Santos, M. Massi, P. M. S. C. M. Leite, C. A. R. Costa, E. M. Lanzoni, R. S. Pessoa and H. S. Maciel, *Surf. Coat. Techno.*, 2014, **260**, 205-213.

20. G. Covarel, B. Bensaid, X. Boddaert, S. Giljean, P. Benaben and P. Louis, *Surf. Coat. Technol.*, 2012, **211**, 138-142.

21. R. Amini and A. A. Sarabi, *Appl. Surf. Sci.*, 2011, **257**, 7134-7139.

22. N. Van Phuong, S. Moon, D. Chang and K. H. Lee, *Appl. Surf. Sci.*, 2013, **264**, 70-78.

23. D. Y. Lee, W. C. Kim and J. G. Kim, *Corrosion Sci.*, 2012, **64**, 105-114.

24. Y. Song, D. Shan, R. Chen, F. Zhang and E.-H. Han, *Surf. Coat. Technol.*,

2009, **203**, 1107-1113.

25. M. A. Smit, J. A. Hunter, J. D. B. Sharman, G. M. Scamans and J. M. Sykes, *Corrosion Sci.*, 2004, **46**, 1713-1727.

26. Y. W. Yao, Y. Zhou, C. M. Zhao, Y. X. Han and C. X. Zhao, *J. Electrochem. Soc.*, 2013, **160**, C185-C188.

27. S. M. A. Shibli and F. Chacko, *Appl. Surf. Sci.*, 2011, **257**, 3111-3117.

Table of contents entry

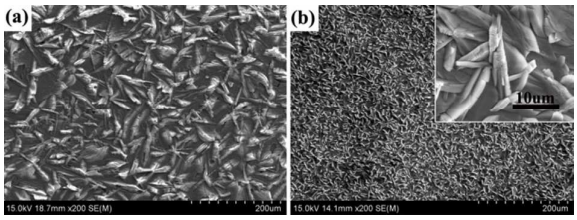

The uniform fine-crystalline structure is exhibited on PCC coating on 35CrMnSi with Fe^{2+} curing (b).